

Predictable patterns of CTL escape and reversion and the limited role of epistasis in HIV-1 evolution

Duncan S. Palmer^{*1,2,9}, Emily Adland³, John A. Frater^{2,4}, Philip J. R. Goulder^{3,5}, Thumbi Ndung'u⁵, Philippa C. Matthews⁴, Rodney E. Phillips^{2,4}, Roger Shapiro^{7,8}, Gil McVean¹, and Angela R. McLean^{2,10}

¹Department of Statistics, 1 South Parks Road, University of Oxford, Oxford OX1 3TG, UK

²Institute for Emerging Infections, The Oxford Martin School, Oxford OX1 3BD, UK

³Department of Paediatrics, University of Oxford, Oxford OX1 3SY, UK

⁴Nuffield Department of Clinical Medicine, Peter Medawar Building for Pathogen Research, University of Oxford, Oxford OX1 3SY, UK

⁵HIV Pathogenesis Programme, Doris Duke Medical Research Institute, University of KwaZulu-Natal, Durban, 4013 South Africa

⁶Ragon Institute of Massachusetts General Hospital, Massachusetts Institute of Technology and Harvard University, Boston, MA 02139

⁷Botswana Harvard AIDS Institute Partnership, Gaborone BO 320, Botswana

⁸Department of Immunology and Infectious Diseases, Harvard School of Public Health, Boston, MA 02215

⁹Wellcome Trust Centre for Human Genetics, Roosevelt Drive, Oxford OX3 7BN, UK

¹⁰Zoology Department, South Parks Road, University of Oxford, Oxford OX1 3PS, UK

Abstract

The twin processes of viral evolutionary escape and reversion in response to host immune pressure, in particular the cytotoxic T-lymphocyte (CTL) response, helps shape Human Immunodeficiency Virus-1 sequence evolution in infected host populations. The tempo of CTL escape and reversion is known to differ between CTL escape variants in a given host population. A wealth of epistatic effects - both intermediary sequence changes on the path to CTL escape and compensatory mutations which restore replicative capacity following viral escape - have been reported. Given the importance of epistatic effects in these processes, we ask: are rates of escape and reversion comparable across infected host populations? For three cohorts taken from three continents, we estimate escape and reversion rates at 23 escape sites in *gag* epitopes. Surprisingly, we find highly consistent escape rate estimates across the examined cohorts. Reversion rates are also consistent between a Canadian and South African infected host population. We investigate the importance of epistasis further by examining *in vitro* replicative capacities of viral sequences with minimal variation: point escape mutants induced in a lab strain. Remarkably, despite the complexities of epistatic effects and the diversity of both hosts and viruses, CTL escape mutants which escape rapidly tend to be those with the highest replicative capacity when applied as a single point mutation. Similarly, mutants inducing the greatest costs to viral replicative capacity tend to revert more quickly. These data suggest that escape rates in *gag* are consistent across host populations and, in general, epistatic effects do not dramatically affect escape rates.

Keywords: HIV-1, escape, CTL, phylodynamics, epistasis

Abbreviations: HIV-1, Human Immunodeficiency Virus-1; CTL, Cytotoxic T-lymphocyte, MCMC; Markov Chain Monte-Carlo

In HIV-1 infected individuals there is a steady arms race between the virus on one side and the host immune system on the other [1]. The Cytotoxic T-lymphocyte (CTL) response is part of the adaptive immune system. Within nucleated cells, cytosolic peptides (both self and non-self) are presented at the cell surface by human leukocyte antigen (HLA) class I molecules [2], encoded by HLA genes; the

*duncan.palmer@stats.ox.ac.uk

most variable loci in the entire human genome [3]. These protein fragments are known as ‘epitopes’ upon presentation. CTLs may recognise epitopes as non-self and destroy the presenting cell. The CTL response can select for mutations within or flanking epitopes which result in reduced immune recognition of virally infected cells. Termed CTL escape mutants, these variants may reduce HLA class I binding affinity, alter epitope processing, or affect T-cell receptor contact sites [4, 5, 6, 7]. Importantly, the repertoire of viral epitopes that may be presented is dependent upon the ‘type’ of the HLA class I molecule. If an epitope can be presented, it is said to be ‘restricted’ by that HLA type, and the host is known as ‘HLA matched’ for that epitope. A host lacking the class I molecule required to present the epitope is known as ‘HLA mismatched’ for that epitope. Viruses bearing escape mutations can be transmitted between hosts [8, 9], and reversion of the infecting virus may take place due to the removal of HLA dependent selection pressure and viral fitness costs of CTL immune escape [10, 11].

The viral population present in a given infected individual reflects the selective environment of the current host as well as the remnants of selection from previous hosts. During the course of HIV-1 infection, viral mutations can open pathways to CTL immune escape or compensate for costs to replicative capacity of such mutations [12, 13, 14, 15, 16]. Methods used to model and parameterise the CTL escape and subsequent reversion often assume that the timings of escape and reversion are governed by behaviour at a single site [17, 18, 19, 20, 21, 22, 23, 24]. This is a clear simplification. In fact, the replicative fitness landscape of HIV-1 is thought to be characterised by strong epistasis [25, 26]. The existence and potential complexity of epistatic interactions, coupled with the diversity in HLA profiles, drug regimes, and viruses within host populations leads to the following questions: can individual escape mutants be characterised as having their own escape and reversion rates in a given population, and are escape and reversion rates consistent across host populations?

The ideal data to answer these questions would consist of longitudinal viral sequence samples starting early in infection from a large number of hosts with known HLA types. However, this is not feasible. Instead, we have developed a method which allows us to use cross-sectional viral sequence data to estimate the rates of escape and reversion at escape sites along the HIV-1 genome whilst accounting for the underlying viral genealogy [18]. Using cross-sectional viral sequence data taken from hosts with known HLA types in distinct infected host populations we may estimate population specific rates of escape and reversion at escape sites within optimally defined [27] epitopes. By comparing the resultant escape/reversion rate estimates we can test their consistency between infected host populations.

We apply our model to *gag* sequence data taken from three cohorts sampled from three continents: HOMER (British Columbia, Canada) [28], SSITT (Switzerland) [29, 10], and Bloemfontein (Bloemfontein, South Africa) [30, 31]. Given the diversity of HIV-1 across infected host populations, we were not expecting to see strong similarities between escape/reversion rate estimates. To our surprise, we find a striking agreement between rate estimates, particularly for CTL immune escape. Furthermore, escape rate estimates are consistent between viral populations with distinct HIV-1 subtypes, where *gag* sequence divergence is as high as $\sim 9.2\%$. We also find consistent reversion rate estimates for the Bloemfontein and HOMER datasets (distinct HIV-1 subtypes, average nucleotide sequence divergence: 8.9%). Given the potential collection of paths through sequence space which could restore replicative fitness for a given escape variant, we find it particularly surprising to observe such a highly significant association between reversion rate estimates. These are important results. They suggest that given information regarding the dynamics of escape and reversion in one region, we may begin to make valid statements about these processes in other parts of the world, even when viral populations and HLA frequencies are substantially different. Our results also raise a further question: in general, how important is epistasis in the processes of escape and subsequent reversion? To address this question, we turn to data gathered from *in vitro* assessments of viral replicative capacity [32]. These estimates use site directed mutagenesis to induce escape variants in an otherwise conserved viral background, so do not reflect epistatic interactions in pathways to escape. We ask: do we observe correlations between our population derived escape or reversion rates, and these *in vitro* replicative capacity estimates? Naively ignoring all epistatic interactions, viral diversity, and assuming that all CTL escapes are equally beneficial to the virus, we would expect that an escape mutation which incurs a small cost to viral replicative capacity to rapidly fix in the host’s viral population. Similarly, an escape mutant

Dataset	SSITT [29, 10]	HOMER [44]	Bloemfontein [30, 31]
Population analysed	Switzerland	British Columbia, Canada	Bloemfontein, South Africa
Cohort size	$n = 133$ Zürich ($n = 29$), Geneva ($n = 26$), Bern ($n = 11$), Basel ($n = 11$) St Gall ($n = 8$), Lugano ($n = 7$) Lausanne ($n = 5$)	$n = 567$	$n = 884$, plasma taken from $n = 278$
Sampling date	2000	Between 1996 and 1999	February - September 2006
Sequences analysed	p17 $n = 38$, p24 $n = 55$	$n = 184$	$n = 198$
Treatment	HAART	ART naive on recruitment, initiated HAART between August 1996 and September 1999	ART naive
Study requirements	Undetectable VL for >6 months, $CD4^+$ count > $300\mu l^{-1}$. no history of non-nucleoside reverse transcriptase inhibitors	≥ 3 antiretroviral drugs	Chronic, plasma taken by $CD4^+$ count, low and high favoured: 96 high ($> 500\mu l^{-1}$), 18 medium ($200 - 400\mu l^{-1}$), 164 low ($< 100\mu l^{-1}$)

Table 1: Summary of three studies from which *gag* sequence data was available. For the SSITT and Bloemfontein datasets the number of sequences analysed is lower than the cohort size through a combination of lack of sequencing of *gag*, and data cleaning. For the HOMER dataset, the number of sequences analysed is lower than the cohort size due to restriction of the analysis to a single (unknown) calendar year, and data cleaning.

which dramatically reduces replicative capacity would be expected to take far longer to reach intra-host consensus (we may make similar intuitive statements regarding reversion). Remarkably, despite these vast simplifying assumptions informing this intuition, we find a significant positive correlation between our SSITT escape rate estimates and *in vitro* replicative capacity, and a significant negative correlation between our HOMER reversion rate estimates and *in vitro* replicative capacity. We find it remarkable to see such correlations between rate estimates measured in a reductionist, *in vitro* replicative capacity assay and a real world population of diverse individuals sharing diverse viruses. We conclude that whatever epistatic effects may be present across the HIV-1 proteome, rates of escape and reversion are largely dictated by the costs and benefits of a individual mutations.

Methods

Cohorts

We consider paired viral sequence and host HLA type data taken from studies carried out in three populations: Switzerland (Swiss portion of the Swiss-Spanish intermittent treatment trial (SSITT) cohort [29, 10]); British Columbia, Canada (HAART observational medical evaluation and research (HOMER) cohort [28]); and Bloemfontein, South Africa [30, 31]. For each dataset bulk sequencing data was available, in which sequences obtained are assumed to represent the intra-host viral consensus sequence. We briefly outline the studies and portions of datasets used in Table 1. For each dataset, we restrict our attention to *gag* and to the subset of sequences with the majority subtype in each population as assessed using RIP [33] (software in which sequences are compared to subtype representatives in a sliding window along the viral sequence to identify viral subtype and inter subtype recombinants): subtype B for SSITT and HOMER, and subtype C for Bloemfontein. Our reasons are threefold. Firstly, non-synonymous mutations in *gag* are likely to have a detrimental fitness effect as they encode structural proteins that are among the most highly conserved in the viral proteome [34]. Secondly, the most protective HLA alleles are associated with CTL responses to Gag proteins [35, 36, 37]. Finally, site directed mutagenesis followed by replicative capacity assays have been carried out for a large number of known escape variants located in the *gag* gene [32].

Due to issues of confidentiality, we were unable to obtain the year of sequencing for the analysed portion of the HOMER dataset [28]. However, this is not required as we do not require a rescaling to calendar

time (measured in *years*) from *substitutions site*⁻¹ to determine the existence of rank correlations of rate estimates across datasets. The 184 viral sequences which we analyse from HOMER dataset are taken from the year between 1996 and 1999 inclusive in which the largest number of *gag* sequences were obtained. For the SSITT dataset, separate collections of sequences were available for sequences encoding the p17 and p24 proteins in the *gag* gene. There was not a strong overlap between the patient identifiers of these two sequence sets and the number of sequences in the SSITT dataset was the lowest of our three cohorts, so we chose to analyse the two viral sequence regions independently.

Estimating escape and reversion rates

We estimate HLA prevalence using data from the HLA FactsBook [38]. For the Canadian (HOMER) and Swiss (SSITT) datasets, we set the prevalence at the ‘Caucasian’ estimate. For the African data (Bloemfontein, and the collection of cohorts summarised in Table S1), we set the prevalence at the ‘Black’ estimate. Epitopes examined by Boutwell *et al.* represent all optimally defined CTL epitopes at the time of publication [27]. Escape mutations within these epitopes were defined based upon a list of HLA-associated HIV polymorphisms identified via statistical association [16, 39]. We define escape as any amino acid changes which occur at the same position as escape mutations provided in Boutwell *et al.* [32]. This is clearly an imperfect definition, but provides a sensible compromise between the clear overestimation of allowing all mutations within an epitope to be defined as escape, and only considering exact mutations validated as escapes *in vitro* [17].

Maximum *a posteriori* (MAP) estimate using our integrated method

Full details of the method are provided in Palmer *et al.* [18]. Briefly, we combine Felsenstein’s tree peeling algorithm with existing phylogenetic software to merge statistical phylogenetic techniques with an ordinary differential equation (ODE) model which captures the processes of transmission, escape, and reversion. By doing so, we are able to use the information contained within the viral genealogy to infer estimates of escape and reversion rates (λ_{esc} , λ_{rev}). There are four key steps in our inference regime:

1. Make the mild assumption that the genealogy and HLA/escape information are conditionally independent given the viral sequence information with the epitope removed.
2. Perform Markov chain Monte Carlo (MCMC) to sample genealogies from the posterior conditional on the viral sequence data with the epitope removed using BEAST [40]. We use a coalescent prior in an exponentially growing population. The growth rate parameter of the infected population is sampled within the MCMC.
3. For each sampled viral genealogy, we determine the posterior density for (λ_{esc} , λ_{rev}). This is achieved through a modification of Felsenstein’s peeling algorithm [41].
4. By averaging over tree specific posteriors, we obtain a consensus posterior density for (λ_{esc} , λ_{rev}).

Purely ODE based, naive model

To analyse a particularly large fourth dataset for which rate estimation under our integrated model is not computationally feasible, we turn to a simpler compartment based ordinary differential equation (ODE) model of Fryer *et al.*. For each escape variant under consideration, viral sequence/HLA genotype pairs are split into four classes: HLA mismatched without escape, HLA mismatched with escape, HLA matched without escape and HLA matched with escape. Given these four proportions for an escape site, we then determine a best fit for λ_{esc} and λ_{rev} under the model described in Fryer *et al.* [17] during the exponential growth phase of the epidemic. Best estimates are determined using BFGS [42], an approximation to Newton’s method of hill climbing. Time of the start of the epidemic is set at the time to the most recent common ancestor of a BEAST run on the *gag* sequence data for each dataset.

For a collection of 23 Gag epitopes, we had access to both sequence data and an *in vitro* estimate of viral replicative capacity [32]. Estimates of time to escape/reversion could not be obtained when no individuals in the cohort possessed the restricting HLA. When an escape mutation residing in an epitope reaches consensus in the population, the variant peptide is known as a negatope [43, 44]. Negatopes of HIV-1 subtype B as reported in Boutwell *et al.* [32] are highlighted in Tables S2 - S4 by asterisks.

In vitro viral replicative capacity

We wish to investigate whether there is an association between estimates of escape and reversion rates from host population data and *in vitro* data describing viral replicative capacity. In Boutwell *et al.* [32], the fitness cost of an escape variant is approximated by determining the *in vitro* replicative capacity of the escape mutant inserted into a subtype B lab strain, in the absence of any other sequence variation. The measure of fitness is essentially the exponential *in vitro* growth rate of an isolate relative to the lab strain. Full details of the procedure are provided in [32]. We use these published replicative capacity assay measurements for 23 *gag* escape variants where both viral sequence data and the relevant HLA locus information was available in all three cohorts.

Results

We apply our integrated model [18], and purely ODE based model [17] to data from the SSITT, HOMER and Bloemfontein cohorts. Detailed results, together with estimated replicative capacity of escape variants as previously estimated by an *in vitro* assay [32] are shown in Tables S2, S3 and S4 for the HOMER, SSITT and Bloemfontein datasets respectively. Figure S1 summarises the data for all three regions. For each escape site we determine the proportion of HLA matched hosts harbouring the viral escape form. We perform the same calculation for HLA mismatched hosts. These two values for each of the 23 escape sites are plotted against each other in Figure S1. The majority of the points lie below $y = x$, suggesting that selection for escape is taking place in the majority of the HLA/epitope pairings.

Throughout our results, estimates of time to escape and time to reversion for the HOMER dataset are given in units of *substitutions site*⁻¹. This is because the date of sampling not available due to issues of confidentiality, and thus a scaling from *substitutions site*⁻¹ to *years* could not be estimated using BEAST [45]. Throughout our results, we report the Spearman rank correlation coefficient. We choose this statistic as variance in rate estimates increases drastically as the true underlying rates tend to infinity (or zero if we use a log scale). Also, when comparing replicative capacity to rate of escape or reversion, it is unclear *a priori* that any such relationship would be linear. In each plot, epitopes are abbreviated by writing the first amino acid of the epitope, followed by last, followed by the epitope length (e.g KRWILGLNK → KK10).

Are rates of escape in HLA matched hosts and rates of reversion in HLA mismatched hosts for different epitopes consistent across infected populations in different parts of the world?

Escape rates

Figure 1A-1C shows scatter-plots of estimates of average time to escape for the different combinations of populations: HOMER vs. SSITT, HOMER vs. Bloemfontein, and SSITT vs. Bloemfontein respectively. We find a remarkable positive correlation between escape rate estimates for the SSITT and HOMER cohorts ($\rho = 0.825$; $p = 0.0000135$). We do not find clustering of HLAs of similar prevalence in any portion of the space of times to escape suggesting that the observed correlation is not an artefact

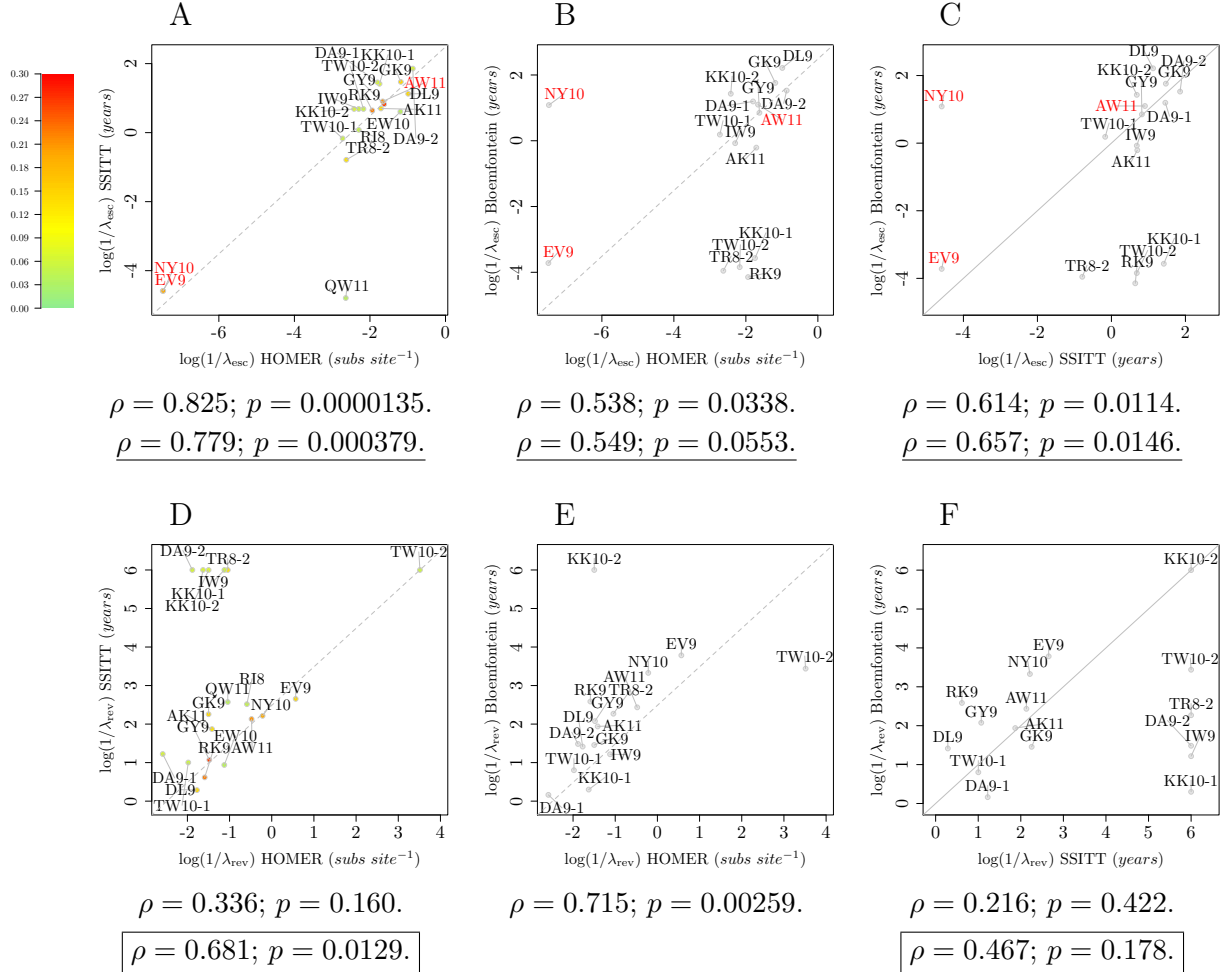


Figure 1: **Comparing estimated times to escape/reversion in each pair of cohorts.** Figures 1A - 1C show MAP estimates of time to escape for the SSITT vs. HOMER, Bloemfontein vs. SSITT and Bloemfontein vs. HOMER MAP estimates respectively. Figures 1D - 1F show the corresponding MAP estimates of times to reversion. Underlined Spearman rank correlation coefficients and p -values are obtained after removal of negatopes, highlighted in red. Boxed Spearman rank correlation coefficients and p -values are evaluated after removal of estimated times to reversion in the SSITT dataset of $\geq 10^6$ years. Numbers following a dash refer to the ordering in Tables S2 - S4, as some epitopes have more than one escape mutation and/or associated restricting HLA. The scale bar indicates the HLA prevalence taken from the HLA handbook [38] for each of the restricting HLA types associated to escape in Caucasian populations. $y = x$ is plotted in solid grey where estimates are on the same timescale. Dotted grey lines represent an estimate of $y = x$ after a change of timescale assuming the Swiss and Canadian epidemics are expanding at roughly the same rate.

of the HLA prevalence in the two populations. We also observe significant positive correlations between estimates of average time to escape for the remaining population combinations in which HIV-1 subtypes are distinct (analysed SSITT and HOMER viral sequences are subtype B, analysed Bloemfontein viral sequences are subtype C): HOMER vs. Bloemfontein: $\rho = 0.538$; $p = 0.0338$, and SSITT vs. Bloemfontein: $\rho = 0.614$; $p = 0.0114$. These results suggest that escape rates are comparable across infected host populations.

In determining the strength of positive correlation between escape rate estimates across populations, we note that a potential source of bias is the inclusion of negatopes: any mutation at high prevalence across hosts will result in a high escape rate estimate, and consequently may lead to spurious associations. To determine if this is the case in our data we remove negatopes (highlighted in red in Figure 1), and re-evaluate correlation coefficients and p -values. In all but HOMER vs. Bloemfontein, we find that positive correlations remained significant (HOMER vs. SSITT: $\rho = 0.779$; $p = 0.000379$, HOMER vs. Bloemfontein: $\rho = 0.549$; $p = 0.0553$, and SSITT vs. Bloemfontein: $\rho = 0.657$; $p = 0.0146$).

A potential source of error in our Bloemfontein escape rate estimates was the low number of individuals in the Bloemfontein dataset with the restricting HLA (shown in Table S3), due to the rarity of these HLA genotypes in African populations coupled with the limited size of the dataset. Additionally, some escape mutations are found at 100% prevalence or are not present at all in the Bloemfontein dataset. 9/20 rate estimates are obtained from data for which just one individual has the restricting HLA, or 0%/100% of HLA matched hosts have the escape mutation. Such escape proportions in HLA matched hosts result in a lack of power to estimate escape rates and can lead to spurious rate estimates [18] (they may lead to estimates of \sim instantaneous escape or \sim infinite time to escape). To attempt to correct for this source of error we obtained a far larger dataset of African sequences coupled with host HLA genotype data [46, 47, 48, 49, 50, 30, 51, 52]. Unfortunately, such a large dataset was computationally intractable using our integrated model. We therefore turn to the simpler ODE model of Fryer *et al.*, noting the previously reported agreement between escape rate estimates derived with our integrated method and this compartment based ODE approach [18]. This is also the case for the data examined here, as shown in Figure S2: the positive correlations between escape rate estimates derived using the two different methods for each population are highly significant. The large dataset summarised in Table S1 is not a single study in a single homogeneous mixing population. Nevertheless, we apply the ODE method to the all of the data in Table S1. We note that there is agreement between MAP estimates of time to escape using the Bloemfontein dataset and the ODE based estimates derived from the entirety of the African dataset in Figure S3 ($\rho = 0.861$, $p = 0.00000223$). Scatterplots of estimates of time to escape using the naive ODE method on the large African dataset against the two HIV-1 subtype B datasets are shown in Figures S4. In both cases we find significant positive correlations ($\rho = 0.711$, $p = 0.00193$ and $\rho = 0.765$; $p = 0.000351$ for African against HOMER and African against SSITT time to escape estimates respectively) which remained significant after removal of negatopes (African vs. HOMER $\rho = 0.723$; $p = 0.00481$, African vs. SSITT $\rho = 0.819$; $p = 0.000340$). We also note that the strongest disagreement seen in the plots occurs when time to escape is very low in one or other of the populations. This occurs when the escape mutation is at high prevalence in one or other of the populations: possibly as a result of founder effects.

Reversion rates

Figures 1D-1F and S5 show the corresponding scatterplots of estimates of time to reversion. We find a striking agreement between the ordering of HOMER and Bloemfontein reversion rate estimates ($\rho = 0.715$, $p = 0.00259$). This correlation was not repeated in any of the other combination of the analysed cohorts. We note that TLYCVHQR, [A]ISPRTLNAW, DRFYKTLRA, KRWIILGLNK, and KRWIILGLNK are estimated to have extremely low reversion rates when using the SSITT data. This is possibly due to the small cohort size and the inherent difficulty in estimating reversion rates (indeed, removal of these potential outliers leads to significant associations between reversion rate estimates between the SSITT and HOMER datasets ($\rho = 0.681$, $p = 0.0129$), though this would have to be checked using a larger European HIV-1/HLA dataset).

Sequence divergence within and between cohorts

The consistency between escape rate estimates in three different populations seems to suggest that epistatic interactions are generally secondary effects during CTL immune evasion. If they weren't, then we would expect such effects to mask positive correlations between escape rate estimates across host populations. To investigate the importance of epistasis, we first examine the viral sequence similarity within and between the SSITT, HOMER, and Bloemfontein cohorts. Nucleotide and amino acid sequence divergence as measured by Hamming distance is shown in Figure S8. We determine this metric for the region of *gag* over which we had the largest number of available sequences. This was to avoid biasing through differences in sequence diversity across *gag*. A neighbour joining tree using the K81 model [53] is shown in Figure S9. Taken together, Figures S8 and S9 show a dramatic divergence between the subtype B and C sequences, as we would expect. We observe mixing of lineages between Canada and Switzerland, coupled with examples of cohort specific clades.

The consistent and significant positive association between escape rate estimates exists despite a mean divergence of up to 9.2% (between the Bloemfontein and SSITT datasets). We also observe a significant positive correlation between reversion rate estimates between the HOMER and Bloemfontein datasets (mean divergence 8.9%), but this does not reach significance for other pairwise comparisons of analysed host populations.

Escape and reversion rates within cohorts vs. *in vitro* replicative capacity estimates

To examine the importance of epistasis further, we consider the most extreme case: complete removal of all sequence variation except at the site of the escape variant. We compare *in vitro* replicative capacity of site directed mutants with our escape and reversion estimates. For a collection of 23 epitope variants we had access to sequence data and an estimate of replicative fitness cost from Boutwell *et al.*, in which site directed mutagenesis was applied to a subtype B lab strain. We first examine the correlation between this *in vitro* measure of replicative capacity and rate estimates in the two populations in which subtype B is the predominant subtype.

Subtype B: Escape and reversion rate estimates in SSITT and HOMER datasets vs. *in vitro* replicative capacity estimates

If we naively assume an absence of epistasis and that the benefit of evading CTL mediated immunity is equal for all escape variants, then we would expect to see average time to escape negatively correlated with *in vitro* replicative capacity, and average time to reversion positively correlated with *in vitro* replicative capacity. Results are displayed in Figure 2. Surprisingly, despite these naive assumptions we indeed observe a negative correlation between time to escape and replicative capacity for the Spearman rank correlation coefficients which reaches significance for the SSITT data ($\rho = -0.451$, $p = 0.0461$). We also observe a positive correlation between time to reversion and replicative capacity which reaches significance for the HOMER data ($\rho = 0.530$, $p = 0.0163$). These findings again suggest that epistatic effects are generally secondary to either the benefits to the virus of CTL escape in HLA matched hosts, or the detriment to viral replicative capacity in HLA mismatched hosts. Such effects appear to be overwhelmed by the impact of insertion or removal of escape mutants. Logically, if epistasis dramatically affected the available pathways to escape/reversion then we would not expect to see time to escape or reversion correlate (negatively and positively respectively) with viral replicative capacity experiments which disregard all sequence variation aside from the escape mutant. Finally, we note that outliers in the Figure 2C are exactly those discussed in the previous section. Removal of these points results in a significant correlation between reversion rate and *in vitro* replicative capacity for the SSITT data ($\rho = 0.810$, $p = 0.000449$). Again we emphasise that larger European sequence datasets with host HLA information should be analysed to determine the accuracy of the reversion rate estimates for these outliers.

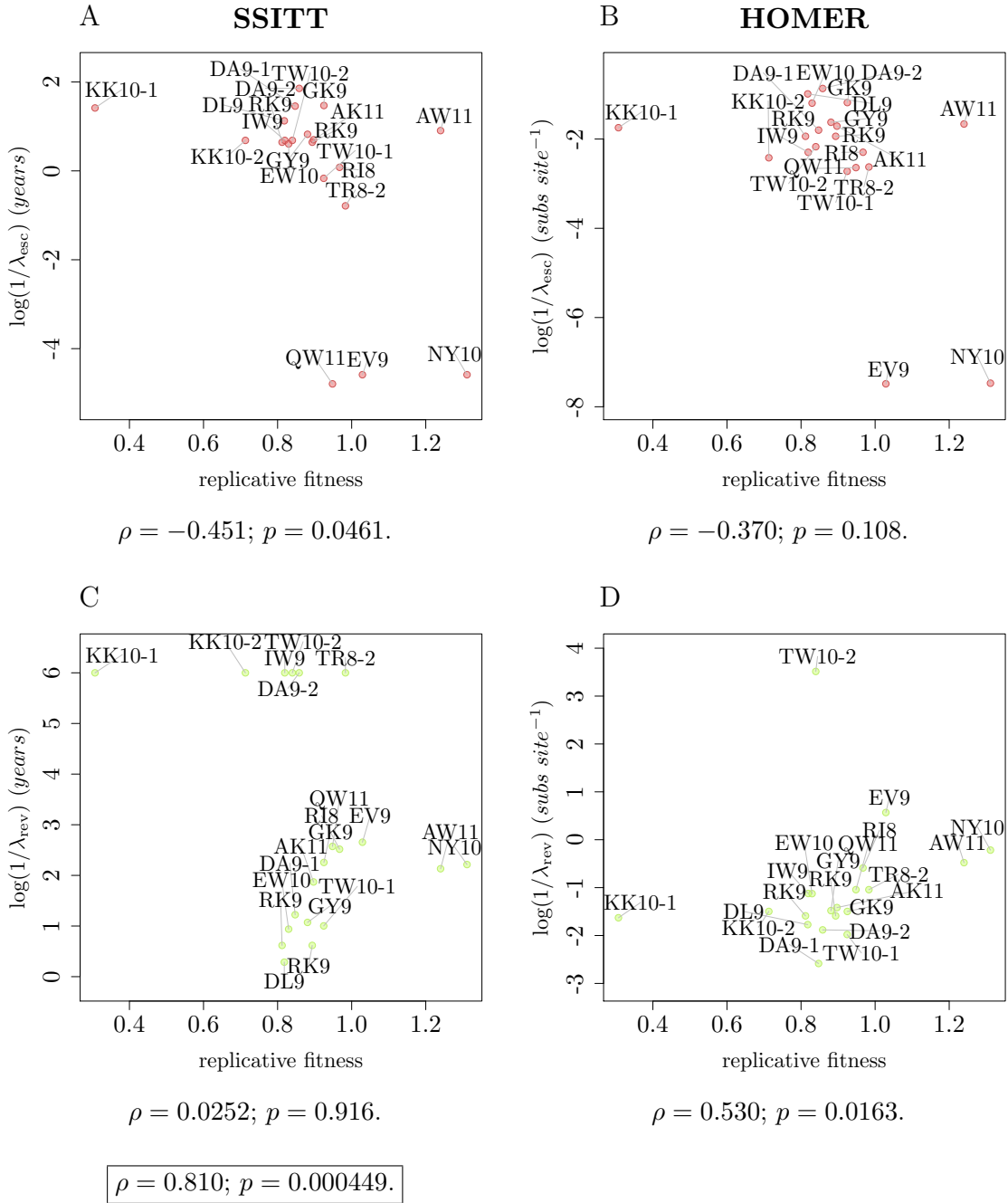


Figure 2: **Replicative capacity plotted against the MAP estimates of time to escape and reversion.** The first and second columns display estimates obtained using *in vivo* data from Switzerland (SSITT) and Canada (HOMER) respectively. Numbers after the epitope abbreviation refer to the ordering in Tables S2 - S4, as some epitopes have more than one escape mutation and/or associated restricting HLA. Time to escape is measured in *years* except in the case of the HOMER cohort in which it is measured in units of substitutions. Spearman rank correlation coefficients; ρ , with associated p -values are displayed on each plot. Boxed Spearman rank correlation coefficients and p -values are evaluated after removal of estimated times to reversion in the SSITT dataset of $\geq 10^6$ *years*.

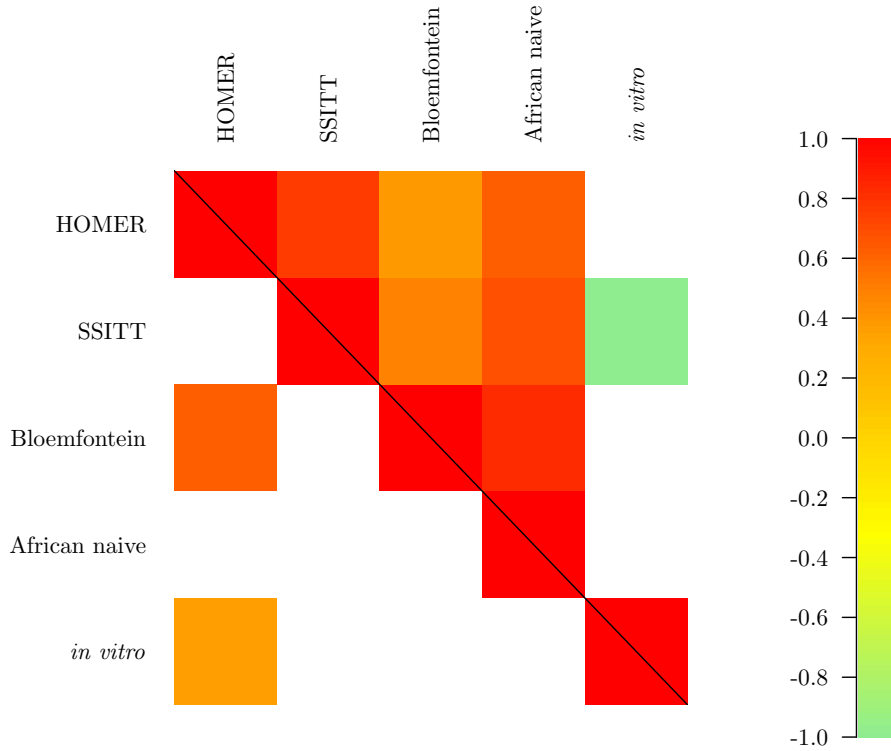


Figure 3: **Summary of all associations.** Significant Spearman rank correlations ($p < 0.05$) between expected time to escape across cohorts and with *in vitro* replicative capacity are shown above the leading diagonal. Significant correlations between reversion rates across cohorts and with *in vitro* replicative capacity are shown below the leading diagonal. Significant Spearman rank correlation coefficients are coloured according to the colour-bar, non-significant associations are shown in white.

Subtype C: Escape and reversion rate estimates in the Bloemfontein dataset vs. *in vitro* replicative capacity estimates

Given the correlation observed between *in vitro* replicative capacity and escape rate in two datasets taken from populations where subtype B is the predominant HIV-1 subtype, we sought to determine if this correlation was replicated in the Bloemfontein dataset where subtype C predominates. We do not find any such correlation between estimated time to escape/reversion in Bloemfontein (or the full African dataset using the naive ODE method, see Figure S7) and *in vitro* replicative capacity. This could suggest a role for epistatic interactions, potentially involving sites distinguishing subtypes B and C. However, we note that the similar replicative capacity of measured escape variants and the noise of such assays, coupled with our low power to estimate many of these rates given the rarity of the associated HLA types in African populations could also lead to a loss of signal of association. Furthermore, founder effects and overlapping epitopes associated to other HLA types have the potential to affect our rate estimates.

Discussion

There is a large amount of literature detailing the existence and complexity of pathways to escape, compensatory mutations and other forms of epistasis in HIV-1 [15, 54, 16, 26, 25]. Given this complexity, it is therefore unclear whether the processes of CTL immune escape and reversion can be meaningfully

modelled and parameterised. In this work, we sought to determine if it makes sense to characterise escape variants by an escape and reversion rate, and ask if such rate estimates are consistent across host populations. Remarkably, we found significant consistency between expected time to escape for each cohort combination, even across HIV-1 subtypes where average sequence divergence between viral populations was as high as $\sim 9.2\%$. Consistency in escape/reversion rate estimates across populations lead to the following question: if escape/reversion rates are correlated whilst viral backgrounds are different, what is the role of epistasis in these processes? To test this, we considered estimates of *in vitro* replicative capacity applied to a subtype B lab strain. If we naively assume that all escape mutations have the same impact upon CTL immune evasion, then we would expect CTL escape mutations that are more costly *in vitro* (i.e. that have a lower viral replicative capacity) to escape more slowly in HLA matched hosts and revert more rapidly in HLA mismatched hosts.

The use of *in vitro* replicative capacity of escape variants applied to a lab strain as a measure of the escape variant's fitness averaged over an entire infected population is clearly a vast simplification. Also, our method requires a number of simplifying assumptions [18]. Despite this, we find a significant negative correlation between *in vitro* replicative capacity and estimated time to escape in the Swiss dataset (SSITT), and a significant positive correlation *in vitro* replicative capacity and *in vivo* estimates of time until reversion in the HOMER dataset. For the Bloemfontein dataset (consisting of subtype C HIV-1 sequences), no association was found for either escape or reversion estimates.

During the process of escape and reversion, it appears that epistatic effects are often overpowered by the effect of a single point mutation; giving rise to consistent escape rate estimates across host populations. This result is powerful as it allows us to legitimately inform a null hypothesis when studying a new HIV-1 dataset. Evidence for correlation between reversion rate estimates across populations and with *in vitro* replicative capacity is less clear cut. This may be due to the inherent difficulty in estimating reversion rates. Reliable reversion rate estimates require multiple instances of transmission of escape mutations followed by reversion in an HLA mismatched host, an event which occurs less often than transmission of wildtype at the site(s) under consideration (particularly if the restricting HLA is rare, or the escape rate is relatively low). Indeed, simulation studies show that a lack of data and low underlying reversion rates can lead to dramatic underestimation of the true rate. Despite this, we observe a strong signal of association between the reversion rates estimated using the Bloemfontein data and those estimated using the HOMER dataset. Further, removal of potentially spurious low rate estimates obtained using the SSITT data results in consistency between HOMER and SSITT reversion rates estimates. Removal of these very points also results in a significant positive correlation between time to reversion and *in vitro* replicative capacity. An alternative explanation for the lack of a signal of correlation in reversion rate estimates between cohorts is that epistatic effects are important in a subset of the analysed epitopes. Epistatic effects playing a stronger role in the reversion process does make sense intuitively: on average a viral lineage spends a longer period of time within HLA mismatched hosts (because HLA diversity is so high). Selection to increase replicative capacity acts across the entirety of the viral genome both in the presence and absence of any HLA associated immune pressure (contrast this to CTL associated selective pressure, which is strongest in and around epitopes). The high dimensionality of sequence space would then lead us to expect multiple pathways to a restoration of viral fitness, not all of which may be associated to a simple reversion of the purported escape mutation.

This study has a number of limitations. Throughout we have applied our methods to subtype B and C viral sequence data from Canada, Switzerland, South Africa, Malawi and Botswana. Access to further host HLA information coupled with cross-sectional HIV-1 sequence data would allow us to determine if similar orderings of escape and reversion rates are observed in further infected host populations, potentially harboring viruses with other HIV-1 subtypes. The analysed escape variants are all found in *gag*. It would be interesting to see if our results may be extended to other portions of the HIV-1 genome. The majority of the collection of optimal epitopes studied [27] have been determined using data from European and North American populations, and thus associated HLA types are likely to be found at high or moderate frequencies within these populations. However, differences in HLA allele frequency distributions across the world often makes rate estimation using data taken from other

parts of the world difficult - we sometimes require far larger datasets to obtain rate estimates for escape variants in one region versus another. Datasets with $>\sim 500$ sequences in HIV-1 *gag* become intractable using our integrated method. Ability to incorporate vast host/virus datasets would allow us to determine escape and reversion rate estimates for escape variants associated to rare HLA alleles and obtain more accurate estimates for escape mutations associated to more common alleles whilst accounting for dependency structure inherent in viral sequence data.

Our results are summarised in Figure 3. With enough data, escape rates are consistent across three populations in three different continents and two viral subtypes. We also demonstrate that reversion rates correlate between estimates obtained from a Canadian and South African dataset, though further data are required to determine if this observation is true in general.

Acknowledgments

We thank Zabrina Brumme and Richard Harrigan for access to host HLA and viral sequence data from the HOMER cohort [44].

We thank Christian Boutwell and Todd Allen for sharing raw replicative capacity data used in [32].

We thank Bruce Walker for allowing us access to the Durban study cohort [49, 52].

References

- [1] Roberts HE et al. (2015) Structured Observations Reveal Slow HIV-1 CTL Escape. *PLoS Genet* 11(2):e1004914+.
- [2] Alberts B et al. (2007) *Molecular Biology of the Cell: Reference Edition*. (Garland Science), 5 edition.
- [3] Robinson J et al. (2013) The IMGT/HLA database. *Nucleic acids research* 41(Database issue):D1222–D1227.
- [4] Zhang SCC et al. (2012) Aminopeptidase substrate preference affects HIV epitope presentation and predicts immune escape patterns in HIV-infected individuals. *Journal of immunology (Baltimore, Md. : 1950)* 188(12):5924–5934.
- [5] Draenert R et al. (2004) Immune selection for altered antigen processing leads to cytotoxic T lymphocyte escape in chronic HIV-1 infection. *The Journal of experimental medicine* 199(7):905–915.
- [6] Iversen AK et al. (2006) Conflicting selective forces affect T cell receptor contacts in an immunodominant human immunodeficiency virus epitope. *Nature immunology* 7(2):179–189.
- [7] Goulder PJR, Walker BD (2012) HIV and HLA Class I: An Evolving Relationship. *Immunity* 37(3):426–440.
- [8] Allen TM et al. (2004) Selection, transmission, and reversion of an antigen-processing cytotoxic T-lymphocyte escape mutation in human immunodeficiency virus type 1 infection. *Journal of virology* 78(13):7069–7078.
- [9] Frater AJ et al. (2006) Passive Sexual Transmission of Human Immunodeficiency Virus Type 1 Variants and Adaptation in New Hosts. *J. Virol.* 80(14):7226–7234.
- [10] Frater AJ et al. (2007) Effective T-Cell Responses Select Human Immunodeficiency Virus Mutants and Slow Disease Progression. *Journal of Virology* 81(12):6742–6751.

- [11] Leslie AJ et al. (2004) HIV evolution: CTL escape mutation and reversion after transmission. *Nature Medicine* 10(3):282–289.
- [12] Schneidewind A et al. (2007) Escape from the Dominant HLA-B27-Restricted Cytotoxic T-Lymphocyte Response in Gag Is Associated with a Dramatic Reduction in Human Immunodeficiency Virus Type 1 Replication. *Journal of Virology* 81(22):12382–12393.
- [13] Brockman MA et al. (2007) Escape and Compensation from Early HLA-B57-Mediated Cytotoxic T-Lymphocyte Pressure on Human Immunodeficiency Virus Type 1 Gag Alter Capsid Interactions with Cyclophilin A. *Journal of Virology* 81(22):12608–12618.
- [14] Crawford H et al. (2007) Compensatory Mutation Partially Restores Fitness and Delays Reversion of Escape Mutation within the Immunodominant HLA-B*5703-Restricted Gag Epitope in Chronic Human Immunodeficiency Virus Type 1 Infection. *Journal of Virology* 81(15):8346–8351.
- [15] Kelleher AD et al. (2001) Clustered mutations in HIV-1 gag are consistently required for escape from HLA-B27-restricted cytotoxic T lymphocyte responses. *The Journal of experimental medicine* 193(3):375–386.
- [16] Brumme ZL et al. (2009) HLA-Associated Immune Escape Pathways in HIV-1 Subtype B Gag, Pol and Nef Proteins. *PLoS ONE* 4(8):e6687+.
- [17] Fryer HR et al. (2010) Modelling the Evolution and Spread of HIV Immune Escape Mutants. *PLoS Pathog* 6(11):e1001196+.
- [18] Palmer D, Frater J, Phillips R, McLean AR, McVean G (2013) Integrating genealogical and dynamical modelling to infer escape and reversion rates in HIV epitopes. *Proceedings of the Royal Society B: Biological Sciences* 280(1762).
- [19] Asquith B, Edwards CTT, Lipsitch M, McLean AR (2006) Inefficient Cytotoxic T Lymphocyte-Mediated Killing of HIV-1-Infected Cells In Vivo. *PLoS Biol* 4(4):e90+.
- [20] Asquith B, McLean AR (2007) In vivo CD8+ T cell control of immunodeficiency virus infection in humans and macaques. *Proceedings of the National Academy of Sciences* 104(15):6365–6370.
- [21] Fernandez CS et al. (2005) Rapid Viral Escape at an Immunodominant Simian-Human Immunodeficiency Virus Cytotoxic T-Lymphocyte Epitope Exact a Dramatic Fitness Cost. *Journal of Virology* 79(9):5721–5731.
- [22] Ganusov VV, De Boer RJ (2006) Estimating Costs and Benefits of CTL Escape Mutations in SIV/HIV Infection. *PLoS Comput Biol* 2(3):e24+.
- [23] Goonetilleke N et al. (2009) The first T cell response to transmitted/founder virus contributes to the control of acute viremia in HIV-1 infection. *The Journal of Experimental Medicine* 206(6):1253–1272.
- [24] Ganusov VV et al. (2011) Fitness Costs and Diversity of the Cytotoxic T Lymphocyte (CTL) Response Determine the Rate of CTL Escape during Acute and Chronic Phases of HIV Infection. *Journal of Virology* 85(20):10518–10528.
- [25] Hinkley T et al. (2011) A systems analysis of mutational effects in HIV-1 protease and reverse transcriptase. *Nat Genet* 43(5):487–489.
- [26] Bonhoeffer S, Chappey C, Parkin NT, Whitcomb JM, Petropoulos CJ (2004) Evidence for positive epistasis in HIV-1. *Science (New York, N. Y.)* 306(5701):1547–1550.
- [27] Llano A, Williams A, Olvera A, Silva-Arrieta S, Brander C (year?) Best-characterized hiv-1 ctl epitopes: The 2013 update.
- [28] Brumme ZL et al. (2008) Human leukocyte antigen-specific polymorphisms in HIV-1 Gag and their association with viral load in chronic untreated infection. *AIDS (London, England)* 22(11):1277–1286.

- [29] Fagard C et al. (2003) A prospective trial of structured treatment interruptions in human immunodeficiency virus infection. *Archives of internal medicine* 163(10):1220–1226.
- [30] Huang KHGH et al. (2009) Prevalence of HIV type-1 drug-associated mutations in pre-therapy patients in the Free State, South Africa. *Antiviral therapy* 14(7):975–984.
- [31] Huang KHG et al. (2011) Progression to AIDS in South Africa Is Associated with both Reverting and Compensatory Viral Mutations. *PLoS ONE* 6(4):e19018+.
- [32] Boutwell CL et al. (2013) Frequent and Variable Cytotoxic-T-Lymphocyte Escape-associated Fitness Costs in the Human Immunodeficiency Virus Type 1 Subtype B Gag Proteins. *Journal of Virology* 87(7):3952–3965.
- [33] Siepel AC, Halpern AL, Macken C, Korber BT (1995) A computer program designed to screen rapidly for HIV type 1 intersubtype recombinant sequences. *AIDS research and human retroviruses* 11(11):1413–1416.
- [34] Li B et al. (2007) Rapid Reversion of Sequence Polymorphisms Dominates Early Human Immunodeficiency Virus Type 1 Evolution. *J. Virol.* 81(1):193–201.
- [35] Kiepiela P et al. (2007) CD8+ T-cell responses to different HIV proteins have discordant associations with viral load. *Nature medicine* 13(1):46–53.
- [36] Zuñiga R et al. (2006) Relative Dominance of Gag p24-Specific Cytotoxic T Lymphocytes Is Associated with Human Immunodeficiency Virus Control. *Journal of Virology* 80(6):3122–3125.
- [37] Novitsky V et al. (2003) Association between Virus-Specific T-Cell Responses and Plasma Viral Load in Human Immunodeficiency Virus Type 1 Subtype C Infection. *Journal of Virology* 77(2):882–890.
- [38] Marsh SGE, Parham P, Barber LD (2000) *The HLA FactsBook*. (Academic Press), 1 edition.
- [39] Wang YE et al. (2009) Protective HLA class I alleles that restrict acute-phase CD8+ T-cell responses are associated with viral escape mutations located in highly conserved regions of human immunodeficiency virus type 1. *Journal of virology* 83(4):1845–1855.
- [40] Drummond AJ, Suchard MA, Xie D, Rambaut A (2012) Bayesian phylogenetics with BEAUti and the BEAST 1.7. *Molecular biology and evolution* 29(8):1969–1973.
- [41] Felsenstein J (1981) Evolutionary trees from DNA sequences: A maximum likelihood approach. *Journal of Molecular Evolution* 17(6):368–376.
- [42] Nash JC (1990) *Compact Numerical Methods for Computers: Linear Algebra and Function Minimisation*. (CRC Press), 2 edition.
- [43] Moore CB et al. (2002) Evidence of HIV-1 Adaptation to HLA-Restricted Immune Responses at a Population Level. *Science* 296(5572):1439–1443.
- [44] Leslie A et al. (2005) Transmission and accumulation of CTL escape variants drive negative associations between HIV polymorphisms and HLA. *The Journal of experimental medicine* 201(6):891–902.
- [45] Drummond A, Rambaut A (2007) BEAST: Bayesian evolutionary analysis by sampling trees. *BMC Evolutionary Biology* 7(1):214+.
- [46] Kiepiela P et al. (2004) Dominant influence of HLA-B in mediating the potential co-evolution of HIV and HLA. *Nature* 432(7018):769–775.
- [47] Kawashima Y et al. (2009) Adaptation of HIV-1 to human leukocyte antigen class I. *Nature* 458(7238):641–645.
- [48] Rousseau CM et al. (2008) HLA class I-driven evolution of human immunodeficiency virus type 1 subtype c proteome: immune escape and viral load. *Journal of virology* 82(13):6434–6446.

- [49] Leslie A et al. (2010) Additive Contribution of HLA Class I Alleles in the Immune Control of HIV-1 Infection. *Journal of Virology* 84(19):9879–9888.
- [50] Matthews PC et al. (2011) HLA-A*7401-mediated control of HIV viremia is independent of its linkage disequilibrium with HLA-B*5703. *Journal of immunology (Baltimore, Md. : 1950)* 186(10):5675–5686.
- [51] Shapiro RL et al. (2010) Antiretroviral Regimens in Pregnancy and Breast-Feeding in Botswana. *N Engl J Med* 362(24):2282–2294.
- [52] Matthews PC et al. (2008) Central Role of Reverting Mutations in HLA Associations with Human Immunodeficiency Virus Set Point. *Journal of Virology* 82(17):8548–8559.
- [53] Kimura M (1981) Estimation of evolutionary distances between homologous nucleotide sequences. *Proceedings of the National Academy of Sciences of the United States of America* 78(1):454–458.
- [54] Carlson JM et al. (2012) Widespread Impact of HLA Restriction on Immune Control and Escape Pathways of HIV-1. *Journal of Virology* 86(9):5230–5243.

Dataset	Durban [49, 52]	Mma Bana [51]	Kimberley [50]	Thames valley [50]
Population analysed	Durban, South Africa	Gabarone, Botswana	Kimberley, South Africa	Zimbabwe, South Africa, Malawi and Botswana.
Cohort size	$n = 1218$	$n = 514$	$n = 31$	$n = 102$
Sampling date	1999 - 2006	July 2006 - May 2008	–	–
Sequences analysed	$n = 929$	$n = 321$	$n = 26$	$n = 65$
Treatment	ART naive	ART naive	ART naive	Zimbabwe ($n = 55$), Malawi ($n = 7$), South Africa ($n = 3$). ART naive
Study requirements	Recruited following voluntary counselling and testing in anti-natal or outpatient clinics.	Pregnant women	Postnatal mothers	Southern African subjects attending outpatient HIV clinics in the Thames Valley area of the UK

Table S1: Summary of four African studies from which *gag* sequence data and HLA information was available. In each case, the number of sequences analysed is lower than the cohort size through a combination of lack of sequencing of *gag*, and data cleaning. These data were combined and analysed using the ODE model.

Epitope	HLA	HLA prop	with escape		Time to escape (<i>years</i>)		Time to reversion (<i>years</i>)		Replicative capacity	
			HLA +ve	HLA -ve	ODE	MAP	ODE	MAP	rank	actual
GGKKYK _L K	B*08	0.143	0/5	3/34	288	29.6	> 10 ⁶	180	8	0.925
RLRPGKKK	A*03	0.224	7/11	4/28	3.36	4.41	4.58	4.14	20	0.812
RLRPGKKK	A*03	0.224	7/11	4/28	3.36	4.41	4.58	4.14	12	0.894
GSEELRS _L Y	A*01	0.262	5/10	7/29	9.25	6.66	12.7	11.8	13	0.881
ELRS _L YNTV*	B*08	0.143	5/5	33/34	0.001	0.001	> 10 ⁶	451	3	1.03
[A]TLYCVHQR	A11	0.133	0/3	0/36	—	—	—	—	4	1.02
TLYCVHQR	A*11	0.133	3/3	23/36	0.00257	0.163	50.3	> 10 ⁶	5	0.983
[A]ISPRTLNAW	B57	0.057	1/7	8/31	26.3	4.85	> 10 ⁶	> 10 ⁶	9	0.819
QAISPRTLNAW	A*25	0.042	1/1	16/37	0.00133	0.001	120	373	7	0.948
KAFSPEVIPMF	B*57	0.057	0/6	0/30	—	—	—	—	22	0.387
TPQDLNTML	B*42	0.003	0/0	0/57	—	—	—	—	10	0.903
ETINEEA _E EW	A*25	0.042	1/3	3/54	8.90	4.04	17.4	8.68	17	0.830
TSTLQEIGW	B*57	0.057	7/8	5/49	0.610	0.680	8.19	10.1	18	0.924
TSTLQEIGW	B*57	0.057	4/8	12/49	7.25	4.85	162	> 10 ⁶	16	0.840
NPPIPVEIY*	B*35	0.196	7/7	45/50	0.149	0.001	215	164	1	1.31
KRWIILGLNK	B*27	0.073	2/7	3/49	12.2	26.0	13.4	> 10 ⁶	23	0.307
KRWIILGLNK	B*27	0.073	5/7	7/49	1.92	4.85	12.2	> 10 ⁶	21	0.713
RMYSPTSI	B*52	0.051	2/3	30/54	2.59	1.20	> 10 ⁶	329	6	0.967
DRFYKTLRA	B*14	0.065	0/6	2/51	460	28.6	> 10 ⁶	16.7	15	0.847
DRFYKTLRA	B*14	0.065	1/6	1/51	21.5	71.8	7.33	> 10 ⁶	14	0.858
AEQASQEVKNW*	B*44	0.211	11/13	26/44	2.70	8.06	41.1	135	2	1.24
DCKTILKAL	B*08	0.143	2/8	1/49	13.6	13.4	2.21	1.93	19	0.818
ACQGVGGPGHK	A*11	0.133	4/7	13/50	5.62	5.01	23.2	74.1	11	0.897

Table S2: **Fitness costs of epitopes in Gag: SSITT.** MAP and ODE *in vivo* estimates of escape and reversion rates for the collection of epitopes in [32], obtained using sequence data from the SSITT cohort [29, 10]. Proportions of individuals possessing each HLA type are taken from the HLA factsbook [38]. HLA +ve hosts are those with the restricting HLA type. Time to escape and reversion are estimated using the model developed in [18]. Estimates in italics lie on the boundary of our uniform prior. The lack of an estimate occurs when none of the sampled individuals possessed the restricting HLA allele. Putative subtype B negatopes are labelled with asterisks. Amino acids with square brackets lie outside of the epitope. Replicative capacity rank is the ranking of the replicative capacity of the escape mutant (where 1 is the mutant strain with the highest replicative capacity). Replicative capacity actual is the measured scaling of replicative capacity relative to a subtype B lab strain [32].

Epitope	HLA	HLA prop	with escape		Time to escape (<i>years</i>)		Time to reversion (<i>years</i>)		Replicative capacity	
			HLA +ve	HLA -ve	ODE	MAP	ODE	MAP	rank	actual
GGKKYK ¹ KLK	B*08	0.143	2/21	9/140	0.327	0.0657	> 10 ⁴	0.0318	8	0.925
RLRPGKKK	A*03	0.224	26/35	28/124	0.00743	0.0115	0.0226	0.0257	20	0.812
RLRPGKKK	A*03	0.224	26/35	28/124	0.00743	0.0115	0.0226	0.0257	12	0.894
GSEELRS ¹ LY	A*01	0.262	18/38	30/122	0.0359	0.0238	0.0495	0.0331	13	0.881
ELRS ¹ LYNTV*	B*08	0.143	23/23	149/152	0.00001	0.00001	> 10 ⁴	3.70	3	1.03
[A]TLYCVHQR	A11	0.133	0/23	0/153	—	—	—	—	4	1.02
TLYCVHQR	A*11	0.133	16/19	72/131	0.00707	0.00237	0.256	0.0906	5	0.983
[A]ISPRTLNAW	B57	0.057	1/6	35/151	0.0722	0.00504	> 10 ⁴	0.0755	9	0.819
QAISPRTLNAW	A*25	0.042	3/5	28/161	0.0113	0.00229	0.177	0.0906	7	0.948
KAFSPEVIPMF	B*57	0.057	0/10	0/163	—	—	—	—	22	0.387
TPQDLNTML	B*42	0.003	0/0	1/174	—	—	—	—	10	0.903
ETINEEA ¹ EW	A*25	0.042	0/6	7/171	1.37	0.0639	> 10 ⁴	0.0749	17	0.830
TSTLQEIGW	B*57	0.057	7/8	7/165	0.00185	0.00189	0.0103	0.0105	18	0.924
TSTLQEIGW	B*57	0.057	5/8	29/157	0.0104	0.00673	0.102	3270	16	0.840
NPPIPVEI ¹ Y*	B*35	0.196	23/23	139/147	0.00001	0.00001	> 10 ⁴	0.607	1	1.31
KRWIILGLNK	B*27	0.073	5/14	9/164	0.0266	0.0180	0.0290	0.0235	23	0.307
KRWIILGLNK	B*27	0.073	8/10	18/148	0.00368	0.00381	0.0286	0.0318	21	0.713
RMYSPT ¹ SI	B*52	0.051	1/2	30/163	0.0190	0.00506	0.293	0.258	6	0.967
DRFYKTLRA	B*14	0.065	5/12	1/158	0.0176	0.0158	0.00276	0.00260	15	0.847
DRFYKTLRA	B*14	0.065	1/14	2/159	0.195	0.136	0.0392	0.0131	14	0.858
AEQASQEVKNW*	B*44	0.211	25/26	97/126	0.00292	0.0218	0.276	0.332	2	1.24
DCKTILKAL	B*08	0.143	1/21	5/139	0.653	0.103	> 10 ⁴	0.0169	19	0.818
ACQGVGGPGHK	A*11	0.133	7/21	26/142	0.0565	0.0195	0.167	0.0383	11	0.897

Table S3: **Fitness costs of epitopes in Gag: HOMER.** MAP and ODE *in vivo* estimates of escape and reversion rates for the collection of epitopes in [32], obtained using sequence data from the HOMER cohort [28]. Proportions of individuals possessing each HLA type are taken from the HLA factsbook [38]. HLA +ve hosts are those with the restricting HLA type. Time to escape and reversion are estimated using the model developed in [18]. Estimates in italics lie on the boundary of our uniform prior. The lack of an estimate occurs when none of the sampled individuals possessed the restricting HLA allele. Putative subtype B negatopes are labelled with asterisks. Amino acids with square brackets lie outside of the epitope. Replicative capacity rank is the ranking of the replicative capacity of the escape mutant (where 1 is the mutant strain with the highest replicative capacity). Replicative capacity actual is the measured scaling of replicative capacity relative to a subtype B lab strain in [32].

Epitope	HLA	HLA prop	with escape		Time to escape (years)		Time to reversion (years)		Replicative capacity	
			HLA +ve	HLA -ve	ODE	MAP	ODE	MAP	rank	actual
GGKKYK _L K	B*08	0.094	1/13	8/190	101	57.5	60.1	28.6	8	0.925
RLRPGGKK _K	A*03	0.125	15/15	150/165	0.892	0.001	> 10 ⁶	385	20	0.812
RLRPGGKK _K	A*03	0.125	15/15	150/165	0.892	0.001	> 10 ⁶	385	12	0.894
GSEELRS _L Y	A*01	0.095	12/18	60/180	3.99	7.10	40.8	119	13	0.881
ELRS _L YNTV*	B*08	0.094	13/13	190/191	0.001	0.001	> 10 ⁶	6070	3	1.03
[A]TLYCVHQR	A11	0.029	0/1	5/201	698	67.4	> 10 ⁶	> 10 ⁶	4	1.02
TLYCVHQR	A*11	0.029	1/1	156/196	0.001	0.001	> 10 ⁶	186	5	0.983
[A]ISPRTLNAW	B57	0.078	8/9	39/190	0.639	0.843	14.0	16.4	9	0.819
QAISPRTLNAW	A*25	0.009	0/0	51/198	—	—	—	—	7	0.948
KAFSPEVIPMF	B*57	0.078	2/9	13/191	19.8	67.4	20.9	> 10 ⁶	22	0.387
TPQDLNTML	B*42	0.099	13/41	17/151	13.4	28.6	20.5	84.1	10	0.903
ETINEEAAEW	A*25	0.009	0/0	2/203	—	—	—	—	17	0.830
TSTLQEIGW	B*57	0.078	7/9	16/191	1.26	1.54	5.64	6.35	18	0.924
TSTLQEIGW	B*57	0.078	9/9	187/189	0.001	0.001	> 10 ⁶	2750	16	0.840
NPIPVEIY*	B*35	0.108	2/3	59/199	3.64	12.2	27.4	2130	1	1.31
KRWIILGLNK	B*27	0.029	1/1	3/201	0.001	0.001	1.90	2.00	23	0.307
KRWIILGLNK	B*27	0.029	1/1	13/202	0.001	26.9	8.61	> 10 ⁶	21	0.713
RMYSPTSI	B*52	0.033	0/0	199/201	—	—	—	—	6	0.967
DRFYKTLRA	B*14	0.068	4/19	1/183	15.0	15.7	1.41	1.45	15	0.847
DRFYKTLRA	B*14	0.068	2/18	9/181	54.5	33.5	51.7	30.5	14	0.858
AEQASQEVKNW*	B*44	0.112	18/34	54/163	9.48	12.6	68.2	272	2	1.24
DCKTILKAL	B*08	0.094	0/13	3/186	3060	164	> 10 ⁶	26.0	19	0.818
ACQGVGGPGHK	A*11	0.029	0/1	90/196	31.3	0.618	> 10 ⁶	86.8	11	0.897

Table S4: **Fitness costs of epitopes in Gag: Bloemfontein.** MAP and ODE *in vivo* estimates of escape and reversion rates for the collection of epitopes in [32], obtained using sequence data from the Bloemfontein cohort [30, 31]. Proportions of individuals possessing each HLA type are taken from the HLA factsbook [38]. HLA +ve hosts are those with the restricting HLA type. Time to escape and reversion are estimated using the model developed in [18]. Estimates in italics lie on the boundary of our uniform prior. The lack of an estimate occurs when none of the sampled individuals possessed the restricting HLA allele. Putative subtype B negatopes are labelled with asterisks. Amino acids with square brackets lie outside of the epitope. Replicative capacity rank is the ranking of the replicative capacity of the escape mutant (where 1 is the mutant strain with the highest replicative capacity). Replicative capacity actual is the measured scaling of replicative capacity relative to a subtype B lab strain in [32].

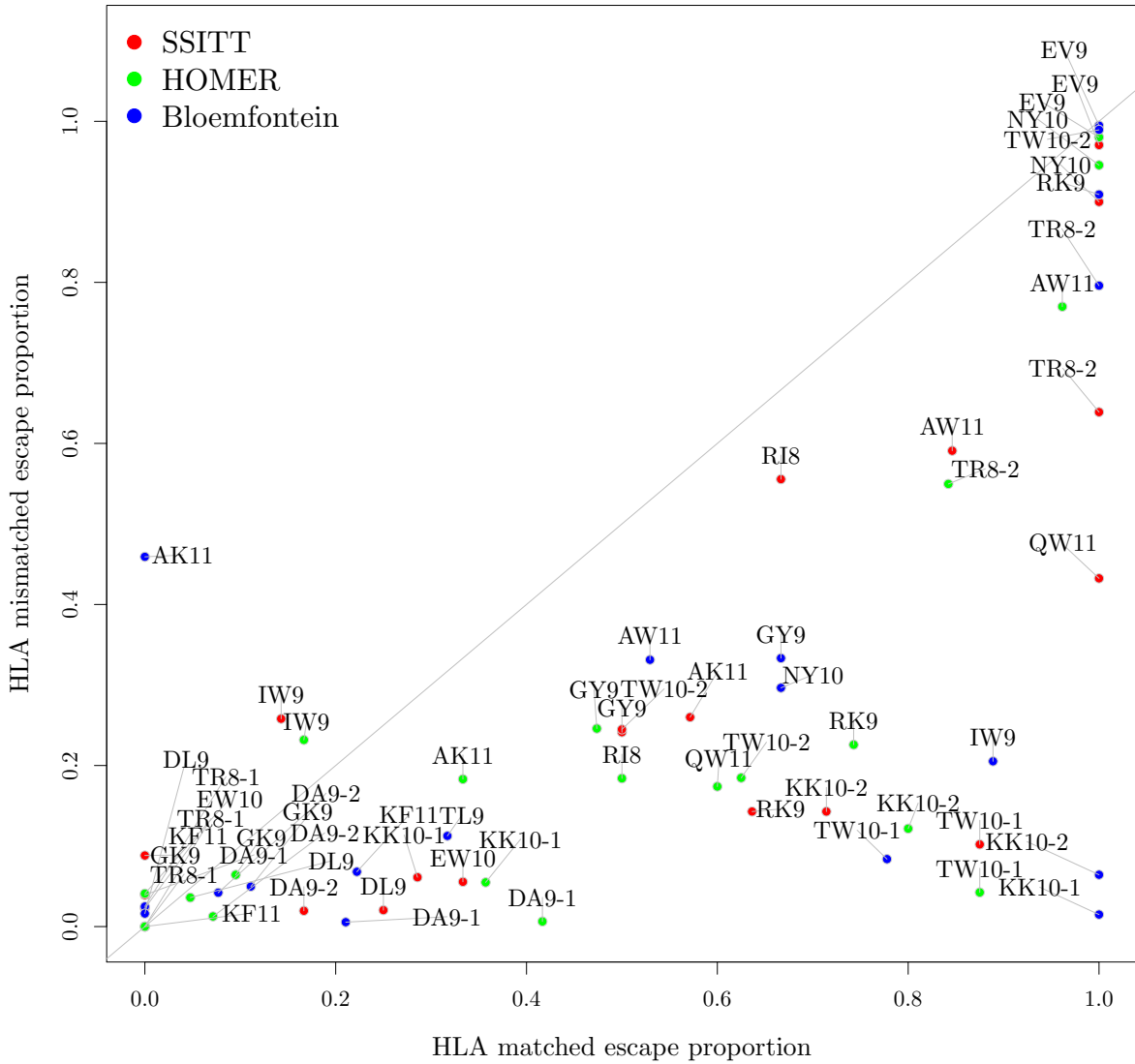


Figure S1: **Scatter-plot of escape proportions in HLA matched and HLA mismatched hosts, coloured by population.** Data points in which no individuals in a population are HLA matched (0/0 escape proportion in HLA matched hosts) were excluded. SSITT, Bloemfontein and HOMER data are shown in red, green and blue respectively. Numbers after the abbreviation of each epitope refers to the ordering in Tables S2 - S4, as some epitopes have more than one escape mutation and/or associated restricting HLA.

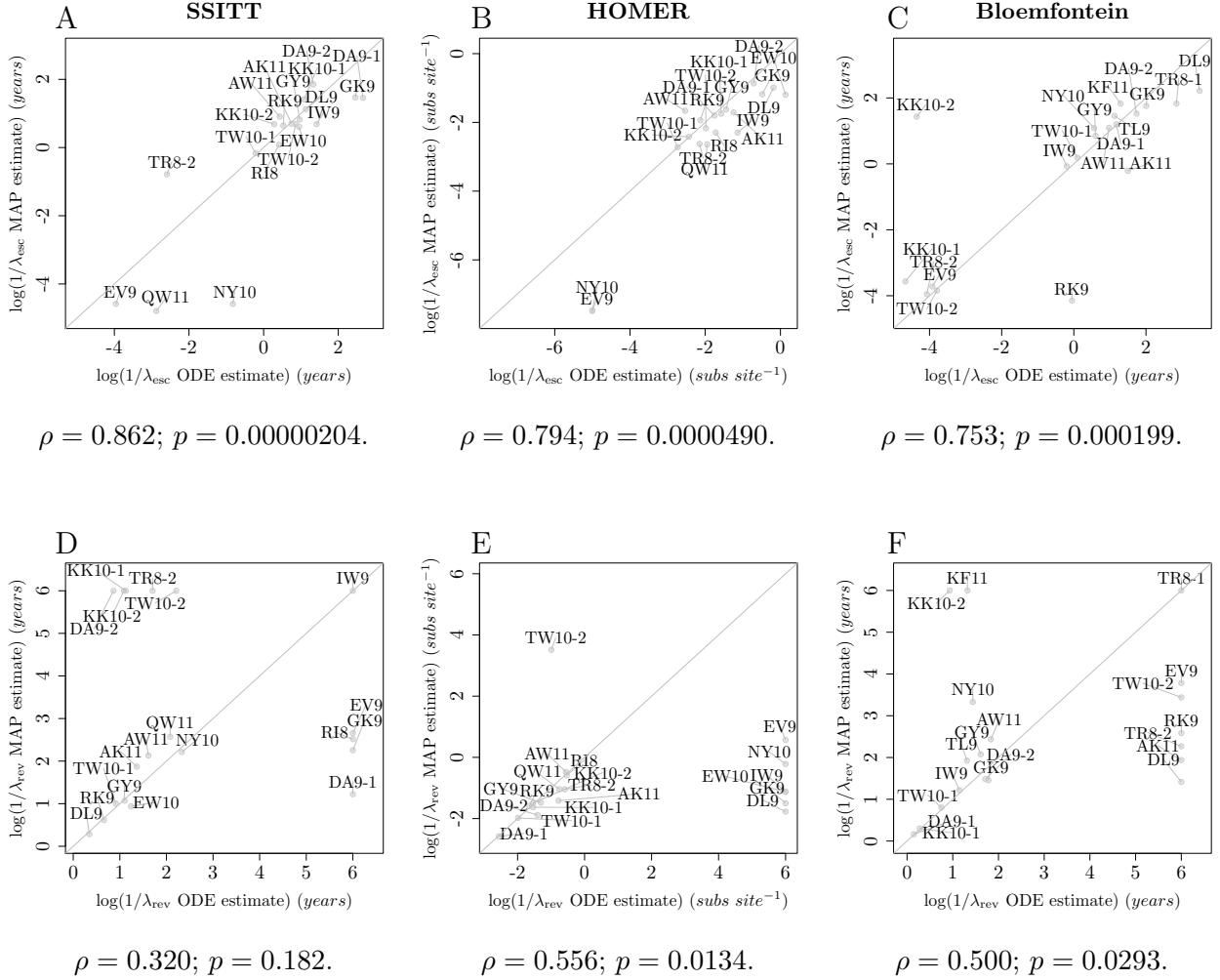


Figure S2: **Comparing MAP estimates of escape/reversion generated under our integrated model to the ODE method of Fryer *et al.* in different populations.** Figures S2A, S2B and S2C show scatter-plots of estimates for time until escape for the two models using data from the SSITT, HOMER and Bloemfontein cohort respectively. Corresponding estimates of the reversion rates using the two methods are shown in Figures S2D - S2F. Spearman rank correlation coefficients (ρ) with associated p -values are displayed. Numbers after the abbreviation of each epitope refers to the ordering in Tables S2 - S4, as some epitopes have more than one escape mutation and/or associated restricting HLA. $y = x$ is plotted in solid grey.

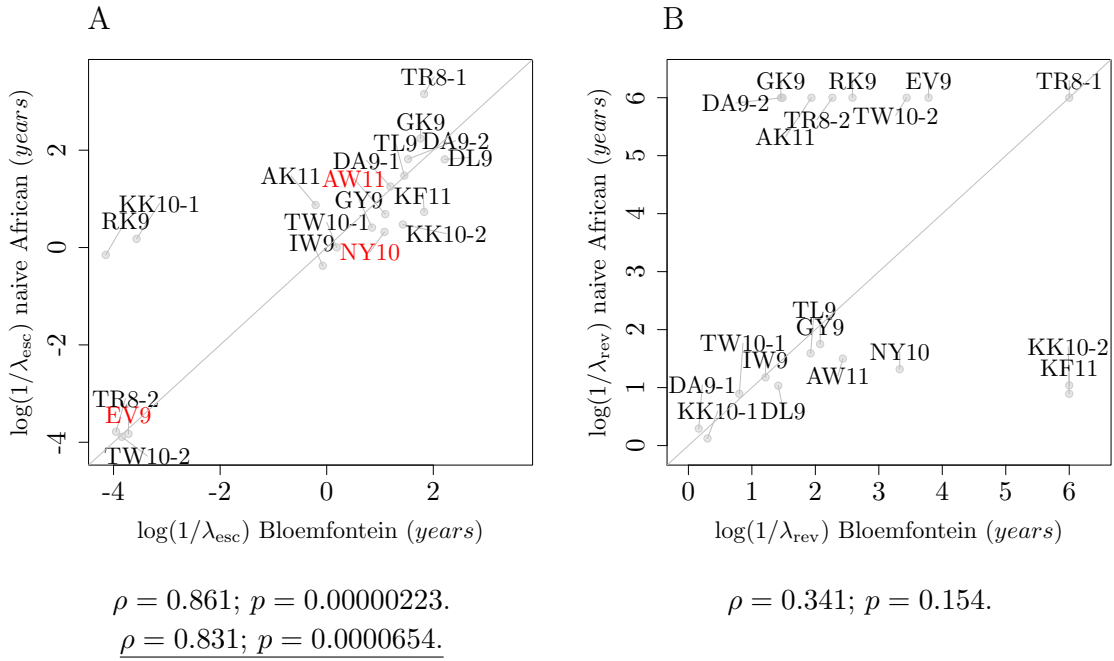


Figure S3: **Comparing time to escape/reversion as estimated from the Bloemfontein data using the integrated method to estimates generated using all available African data and the naive approach.** Spearman rank correlation coefficients (ρ) with associated p -values are displayed. Underlined Spearman rank correlation coefficients and p -values are obtained after removal of negatopes, highlighted in red for estimates of average time to escape. Numbers after the abbreviation of each epitope refers to the ordering in Tables S2 - S4, as some epitopes have more than one escape mutation and/or associated restricting HLA. $y = x$ is shown in solid grey.

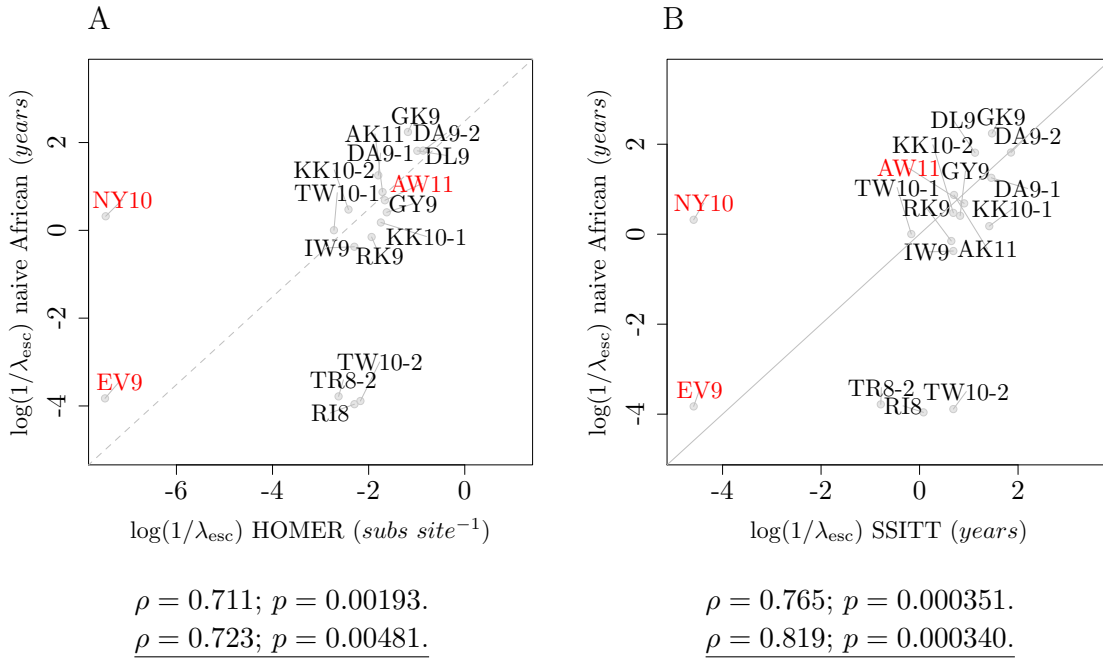


Figure S4: **Comparing time to escape/reversion as estimated from the SSITT/HOMER data using the integrated method to estimates generated using all available African data and the naive approach.** In Figures S4A - S4B SSITT and HOMER MAP estimates are plotted against a naive estimate of the escape rate. Spearman rank correlation coefficients (ρ) with associated p -values are displayed. Underlined Spearman rank correlation coefficients and p -values are obtained after removal of negatopes, highlighted in red. Numbers after the epitope abbreviation refer to the ordering in Tables S2 - S4, as some epitopes have more than one escape mutation and/or associated restricting HLA. We also plot $y = x$ in solid grey where estimates are on the same timescale. Dotted grey lines represent an estimate of $y = x$ after a change of timescale assuming the Swiss and Canadian epidemics are expanding at roughly the same rate.

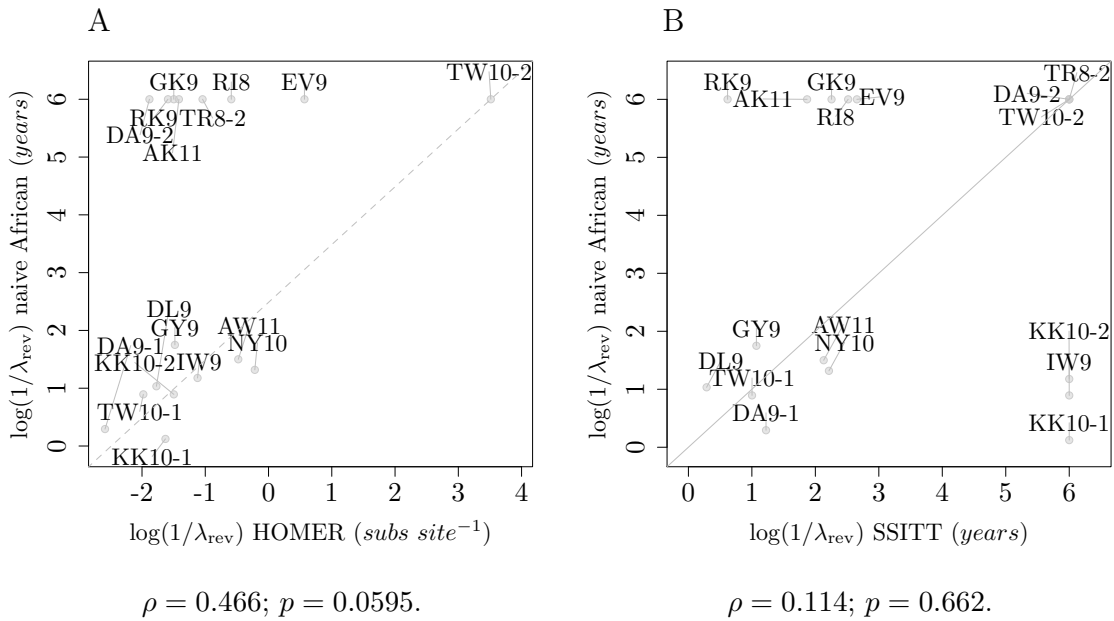


Figure S5: **Comparing time to reversion as estimated from the SSITT/HOMER data to estimates of time to reversion using the large African dataset and the naive approach.** In Figures S5A - S5B SSITT and HOMER MAP estimates are plotted against a naive African estimate of the reversion rate. Spearman rank correlation coefficients (ρ) with associated p -values are displayed. Numbers after the abbreviation of each epitope refers to the ordering in Tables S2 - S4, as some epitopes have more than one escape mutation and/or associated restricting HLA. $y = x$ is plotted in solid grey where estimates are on the same timescale. Dotted grey lines represent an estimate of $y = x$ after a change of timescale assuming the Swiss and Canadian epidemics are expanding at roughly the same rate.

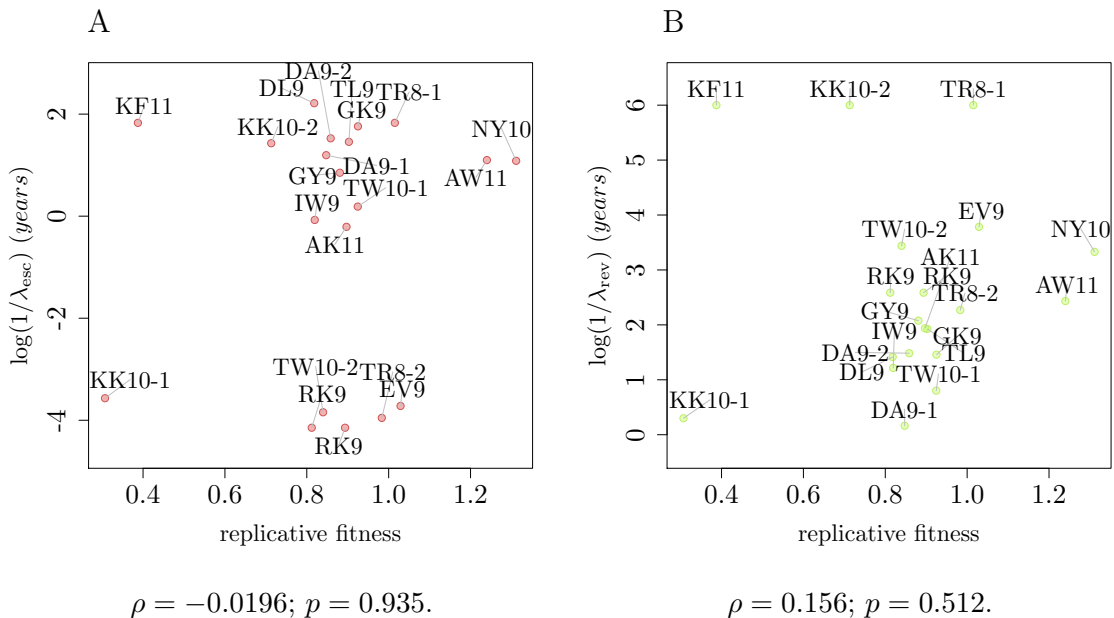


Figure S6: **Scatter-plots of time to escape and reversion estimates against *in vitro* viral replicative capacity: Bloemfontein.** Replicative capacity plotted against the MAP estimates of time to escape is shown in Figure S6A, and the MAP estimates of time to reversion in Figure S6B. Epitopes are labelled by the first three amino acids. Numbers after the abbreviation of each epitope refers to the ordering in Tables S2 - S4, as some epitopes have more than one escape mutation and/or associated restricting HLA. Spearman rank correlation coefficients; ρ , with associated p -values are displayed on each plot.

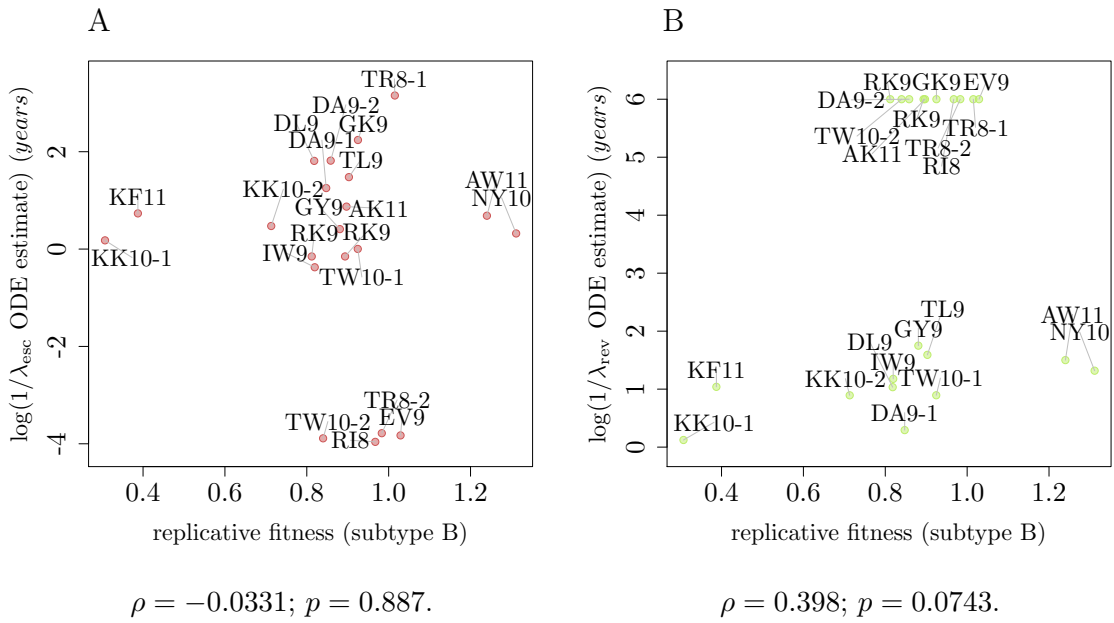


Figure S7: **Scatter-plots of estimates of time to escape and reversion estimated from all African data using naive ODE approach against *in vitro* replicative capacity.** Figure S7A shows a scatter-plot of the respective escape rate estimates. Figure S7B shows the corresponding plot for reversion rate estimates. Numbers after abbreviation of each epitope refers to the ordering in Tables S2 - S4, as some epitopes have more than one escape mutation and/or associated restricting HLA. Spearman rank correlation coefficients with associated p -values are shown.

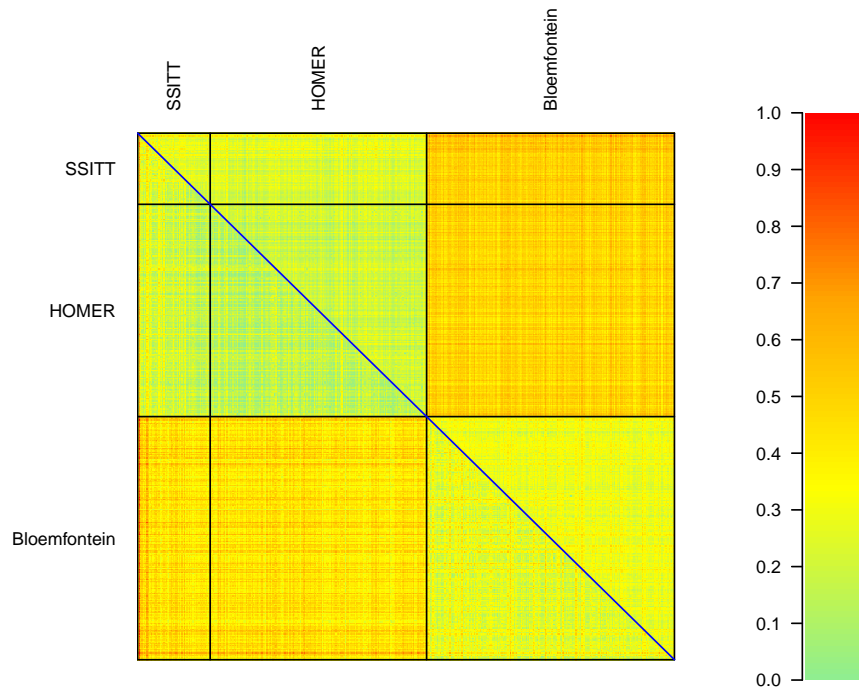


Figure S8: **Sequence divergence by Hamming distance.** We determine the Hamming distance between each pair of sequences in SSITT, HOMER and Bloemfontein for nucleotide and amino acid sequences. We then scale by sequence length to obtain a measure of sequence divergence. Nucleotide sequence divergence is shown above the leading diagonal, and amino acid sequence divergence is plotted below the leading diagonal. Black lines distinguish the SSITT, HOMER, Bloemfontein cohorts. The leading diagonal is shown in blue.

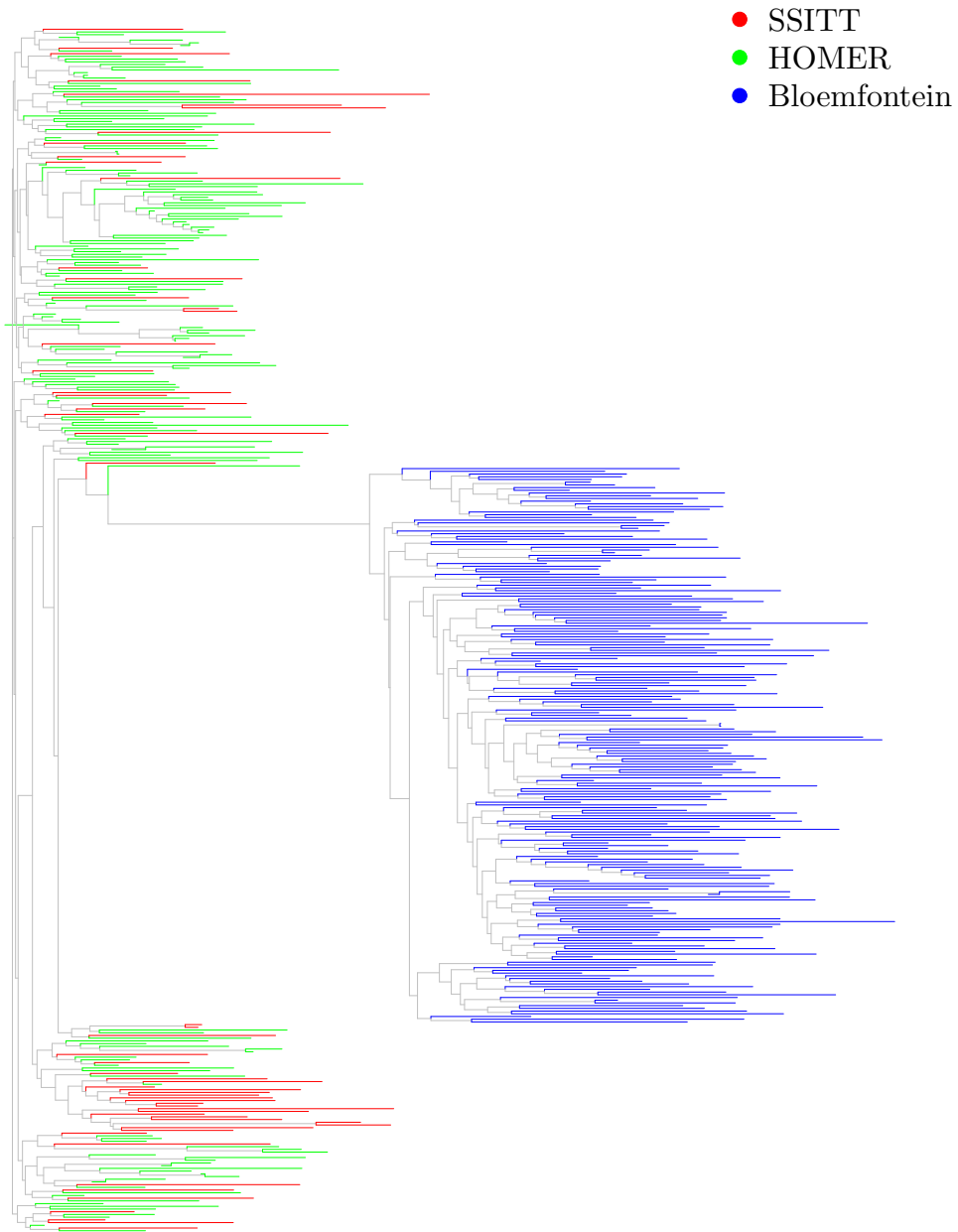


Figure S9: **Neighbour joining tree.** We show a neighbour joining tree obtained using the K81 [53] model applied the largest region of *gag* over which $< 10\%$ sequences contained a gap or an unknown nucleotide in the sequence alignment. Terminal branches are coloured by cohort according to the legend.